

Differential capacitive position sensor for planar MEMS structures with vertical motion

Mark N. Horenstein^{a,*}, Julie A. Perreault^a, Thomas G. Bifano^b

^a Department of Electrical and Computer Engineering, 8 Saint Mary's Street, Boston University, Boston, MA 02215-2421, USA

^b Department of Aerospace and Mechanical Engineering, Boston University, Boston, MA, USA

Received 16 November 1998; accepted 12 July 1999

Abstract

A capacitive sensor has been developed for measuring the vertical deflection of bridge-type micro-electromechanical (MEMS) silicon actuators. The sensor requires no electrodes above the actuator surface and does not require the actuator diaphragm to be used as a signal electrode. Sets of interdigitated electrodes, one for ac signal injection and the other for signal sensing, are placed beneath the actuator membrane. As the actuator deflects, the capacitance between the interdigitated finger electrodes is altered, leading to a change in the time-varying charge induced on the sense fingers. This change in induced charge is monitored by a current-to-voltage converter, thereby providing a measure of actuator displacement in the direction perpendicular to the silicon substrate. Signal voltages on the order of 10 mV per 1 μm of deflection are observed for deflections in the 1- μm range. © 2000 Elsevier Science S.A. All rights reserved.

Keywords: Planar MEMS structures; Vertical motion; Capacitive sensor

1. Introduction

Over the past several years, much progress has been made in the development of micron-sized mechanical devices. Using micro-electromechanical (MEMS) fabrication technology, researchers now routinely make electrostatic motors, actuators, transducers, and other devices. One MEMS structure, the double-anchored, bridge-type flexible beam actuator, shows promise for use in analog optical image processing systems. The typical double-anchored actuator consists of a silicon beam or membrane supported on two sides by rigid walls and insulated from the underlying silicon substrate. Applying a voltage between the membrane and substrate causes the membrane to deflect downward, as in Fig. 1. The deflection becomes a monotonically increasing, cubic-like function of applied voltage. Our research group is presently developing an array of addressable micromachined bridge-type actuators that control a continuously deformable flexible mirror membrane

[1–3]. The principal application of this device is in optical imaging systems. The mirror is supported on posts attached to each actuator as depicted in Fig. 1. The mirror contour is adjusted over vertical distances on the order of an optical wavelength by applying analog voltages to the individual actuators in the array. In our present development tests, deflection of individual actuators is monitored by various optical instruments, including a laser doppler interferometer and a phase sensitive microscope. Although excellent for experimental tests on single actuators, these expensive precision instruments are impractical for monitoring an entire array of actuators such as those that shape the optical imaging mirror. One goal of our research is the development of a simple, easy-to-fabricate system for simultaneously sensing the position of many actuators in a single array.

Most MEMS devices reported to date rely on capacitive sensing techniques for monitoring the position of moving elements [4–7]. The simplest method for monitoring the position of a device such as the bridge-type actuator is to place a capacitively-coupled sense electrode in proximity to the moving element. This method requires that the moving element be used as one of the signal electrodes and not be connected directly to ground. Another more

* Corresponding author. Tel.: +1-617-353-9052; fax: +1-617-353-6440; E-mail: mnh@bu.edu

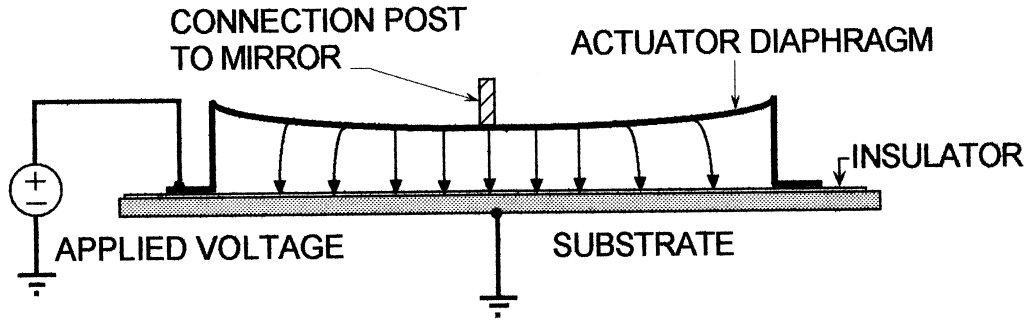


Fig. 1. Actuator diaphragm deflects downward in response to applied voltage.

sensitive technique, the differential capacitance method, is illustrated in Fig. 2. In this case, the moving element is electrically isolated from ground but held at ground potential by the low-impedance input terminal of a current monitoring circuit. Equidistant auxiliary electrodes are placed on either side of the moving element, creating inter-electrode capacitances C_1 and C_2 . The signal electrodes are fed sinusoidal or pulsed signal voltages of equal amplitude and opposite polarity $\pm V_s$; the charge induced on the moving element becomes $(C_1 - C_2)V_s$. With the mechanical element in its equilibrium position, C_1 and C_2 are equal, yielding an induced charge of zero. As the element moves toward one of the signal electrodes, its capacitance relative to that electrode increases while its capacitance relative to the other electrode decreases. The moving element acquires an induced charge proportional to the difference between C_1 and C_2 , leading to a nonzero signal at v_{OUT} .

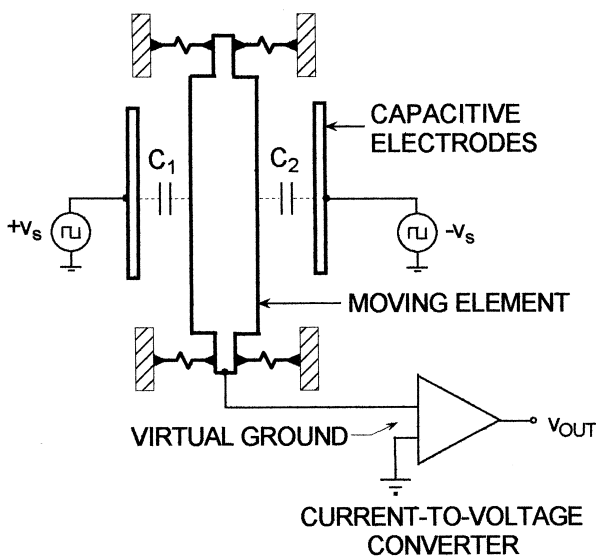


Fig. 2. Essential elements of a differential capacitive position measuring system designed for horizontal motion. Capacitances C_1 and C_2 are functions of the position the moving element. In the equilibrium position, C_1 and C_2 are equal and v_{OUT} equals zero.

The differential capacitance sensing method of Fig. 2 is well suited for MEMS structures involving horizontal motion, but it is not as suitable for elements with vertical motion perpendicular to the substrate surface. In the planar world of MEMS fabrication, vertically-based structures having balanced differential capacitances are not easy to construct. An electrode must be placed both above and below the moving element, requiring additional sacrificial layers and extra masking, photolithography, deposition, and etching steps. Our mirror devices were fabricated using the MCNC multi-user MUMPS batch process [8] in which the additional layers required for differential capacitor sensing of vertically moving structures are simply not available. More importantly, balanced differential capacitance methods are incompatible with our deformable mirror devices. In our structures, an array of many actuators supports a single, optically flawless silicon mirror membrane, and no space is available for placing sense electrodes above each actuator. At the same time, our support post construction configuration causes all the actuator diaphragms in the array to be electrically connected to ground via the optical membrane, thereby preventing the actuator diaphragms from being used as individual signal electrodes. This paper describes an alternative differential capacitive sensing technique in which the moving actuator can be connected directly to ground. Sensing and signal electrodes are fabricated entirely underneath the bridge actuator diaphragm and provide information about actuator deflection. The method relies on the spatially harmonic field distribution produced by the signal electrodes to detect the size of the gap beneath the deflecting actuator. The method has been shown to be reliable, stable, and easy to fabricate.

2. Description of sensing element

The basic features of our capacitive sensing system are shown in Fig. 3, and a photograph of the device taken from a polarizing microscope is shown in Fig. 4. A set of

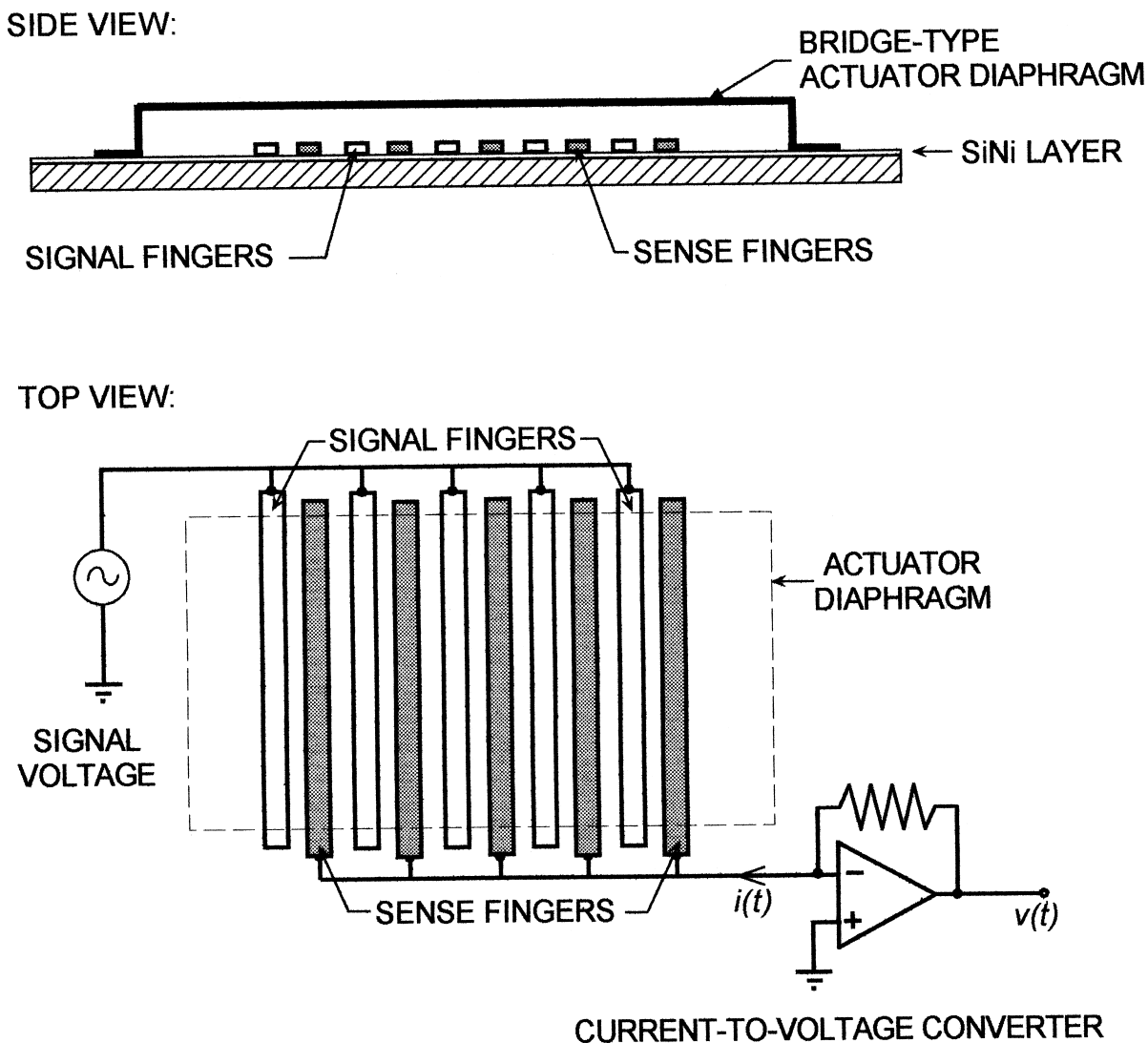


Fig. 3. Basic features of a capacitive vertical position monitoring system based on interdigitated electrodes. The op-amp forms a simple current-to-voltage converter with transconductance gain magnitude equal to R .

two interdigitated electrodes, electrically isolated from each other and from ground, are deposited over a silicon nitride layer beneath the double-anchored bridge. A low-level, time-varying sinusoidal voltage is applied to one group of finger electrodes called the *signal fingers*. The other set of fingers, called the *sense fingers*, is kept at ground potential by the input terminal of a current-to-voltage converter. The magnitude of the sinusoidal voltage applied to the signal fingers is small enough to cause negligible deflection of the actuator, and the frequency of the signal voltage (1 MHz in our case) is low enough that the quasistatic field approximation applies in the actuator gap. In general, if the signal frequency is much smaller than c/l , where l is the largest characteristic dimension of the structure and c the speed of light, then the quasistatic approximation will apply. Under the quasistatic approximation, the field in the actuator gap becomes Laplacian, and the electric field lines produced by the energized signal fingers terminate either

on the sense fingers or on the grounded actuator diaphragm. The total signal field flux terminating on the sense fingers becomes a function of the actuator gap spacing. When the actuator is not deflected, as in Fig. 5a, most of the signal field is coupled to the sense fingers. If the actuator is made to deflect downward, as in Fig. 5b, more signal field lines terminate on the actuator diaphragm, and fewer signal field lines reach the sense fingers. In essence, the deflection of the actuator reduces the capacitance between the sense and signal fingers and increases the capacitance between the actuator diaphragm and the signal fingers. As a consequence, the charge $Q(t)$ induced on the sense fingers due to the signal voltage is reduced as the actuator gap narrows. The value of $Q(t)$, which can be measured by monitoring the current $i(t) = dQ/dt$ flowing to the sense fingers, becomes a measure of actuator deflection. The dc field lines causing actuator deflection are not shown in Fig. 5b.

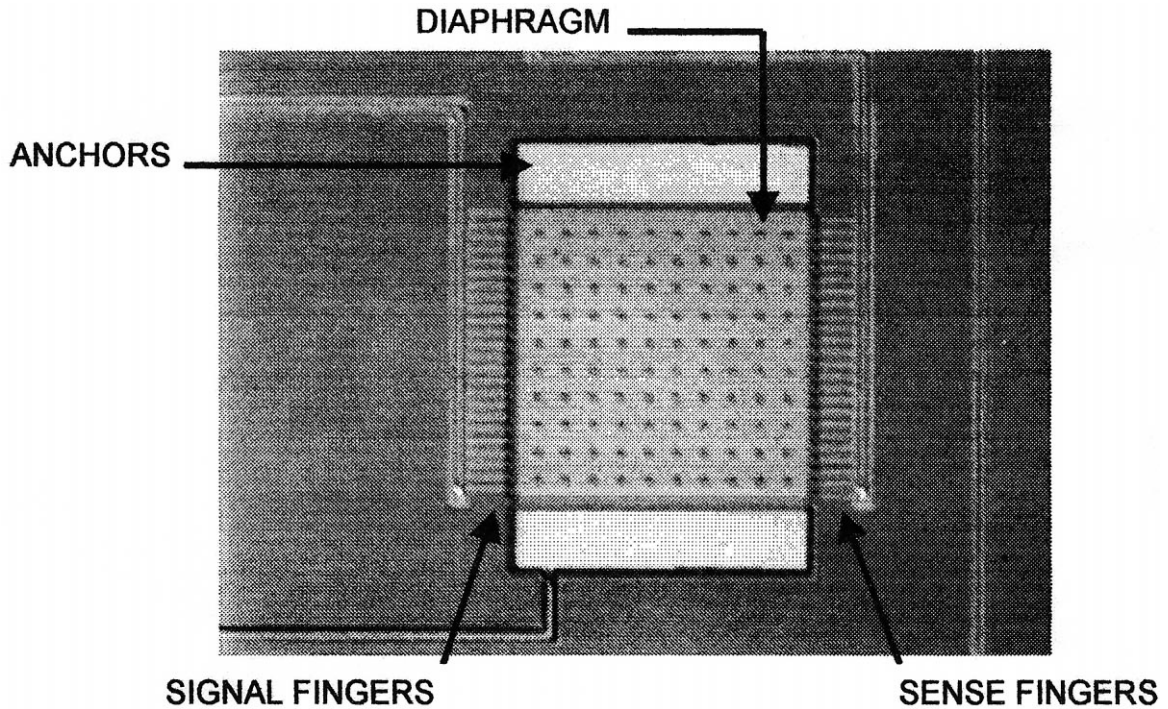


Fig. 4. Photograph of the device taken with a polarizing microscope.

Deflecting the actuator downward requires that an electrostatic field of moderate strength be established between the diaphragm and an underlying electrode plane. In prac-

tice, this deflection field can be produced by adding a dc component to the voltage applied to the signal fingers. The current-to-voltage converter connected to the sense fingers

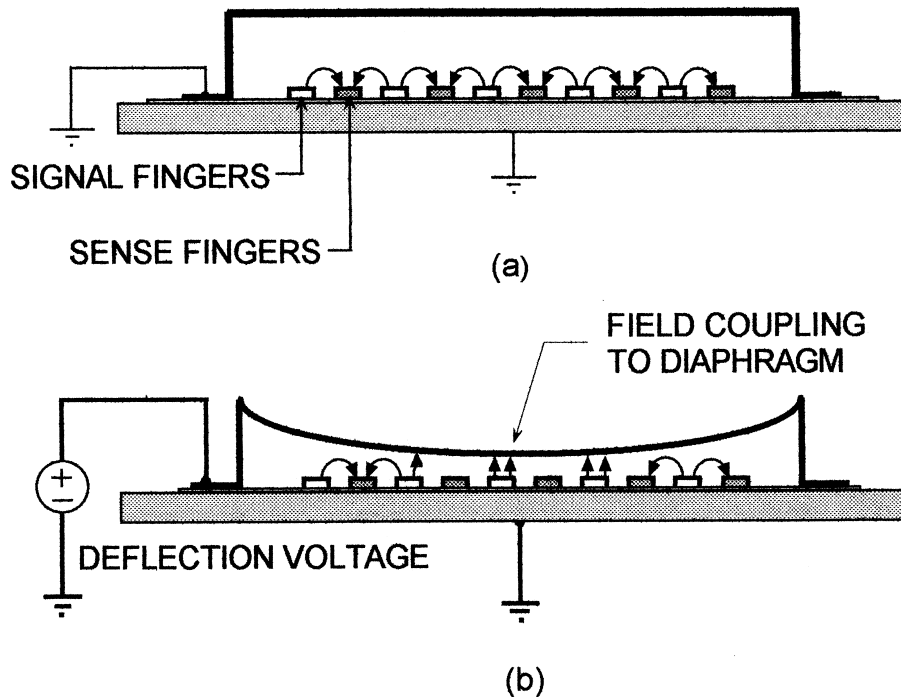


Fig. 5. (a) Actuator at rest with no voltage applied. Signal field coupling between the signal and sense fingers is at its maximum; (b) Actuator deflected downward by the application of a dc voltage. Signal field coupling between the signal and sense fingers is reduced. The dc field lines causing actuator deflection are not shown.

will detect only time varying charge and will not be affected by this dc deflection voltage.

3. Theoretical prediction

The time-varying charge $Q(t)$ induced on the sense fingers is readily predicted from direct calculation if some simplifying assumptions are made. First, for small gap-to-width ratios and deflections, the portion of the actuator diaphragm that resides over the interdigitated electrodes is assumed to be a planar surface even when the diaphragm is deflected from its rest position. This assumption is reasonable for small gap-to-actuator width ratios. Secondly, the finger electrodes are assumed to have no vertical thickness, so that the potential distribution in the plane of the electrodes can be represented by $\Phi(x,t) = f(x)V_s(t)$, where the function $f(x)$ is shown in Fig. 6a, and $V_s(t)$ is the sinusoidal voltage applied to the signal fingers. Note

that $f(x)$ describes the spatial variation of the potential on the electrode plane, and $V_s(t)$ describes the temporal variation.

Because the quasistatic electric field condition applies, the solution for the potential and electric field in the gap can be found by solving a two-dimensional boundary value problem subject to the boundary conditions shown in Fig. 6b. Specifically, the boundary conditions that govern the solution for $\Phi(x,t)$ can be summarized by the following equations:

$$\Phi = f(x)V_s(t) \quad \text{at } z = g \quad (1)$$

and

$$\Phi(x,t) = 0 \quad \text{at } z = 0 \quad (2)$$

where the gap spacing g is measured in the center of the actuator diaphragm, and z is perpendicular to the substrate surface. An analytical expression for $\Phi(x,z,t)$ in the actuator gap region can be found as an infinite series solution to Laplace's equation of electrostatics. In rectan-

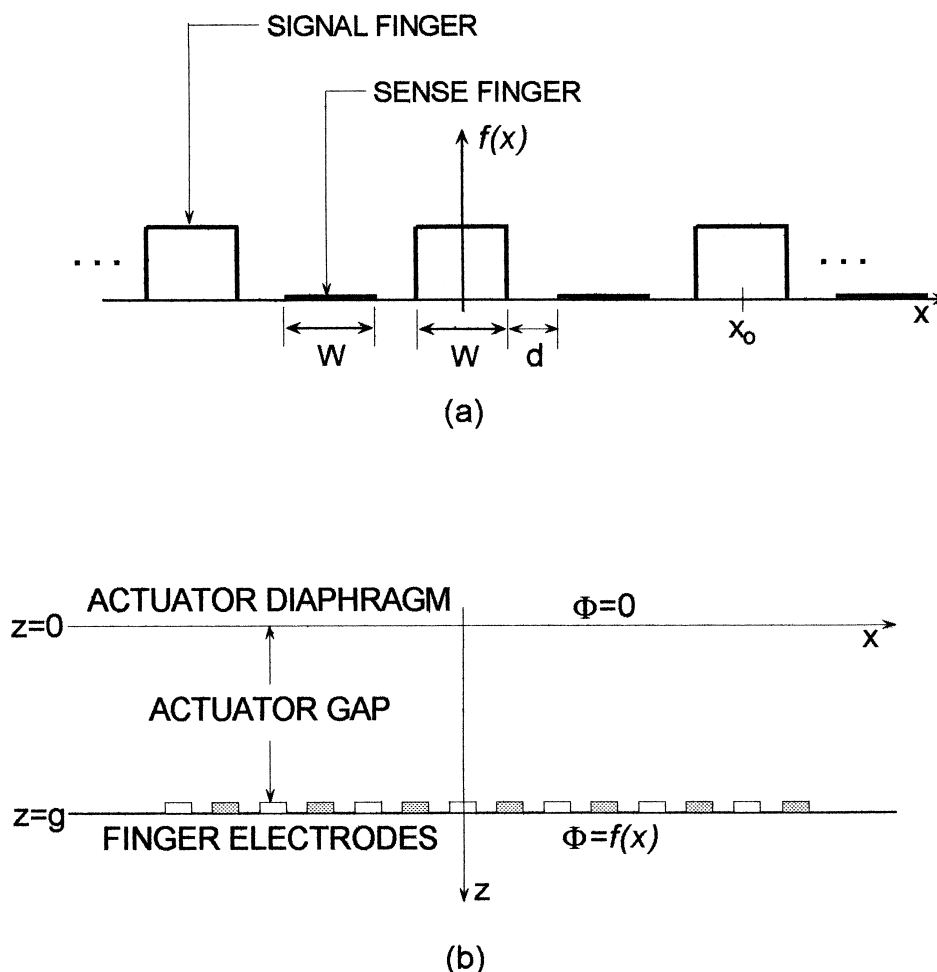


Fig. 6. (a) Potential function $f(x)$ along the x - y plane occupied by the electrodes; (b) Coordinate system for the region between the actuator diaphragm and the interdigitated electrodes.

gular coordinates, the appropriate Laplacian solution form for $\Phi(x, z, t)$ becomes

$$\Phi(x, z, t) = a_0(t) \frac{z}{g} + \sum_{n=1}^{\infty} a_n(t) \cos k_n x \sinh k_n z \quad (3)$$

where $k_n = 2\pi n/x_0$, x_0 is the spatial period of $f(x)$ [9,10], and the $a_n(t)$ coefficients have the dimensions of voltage. The function $\Phi(x, z, t)$ is even in x , as is $f(x)$, and the $\sinh k_n z$ terms force $\Phi(x, z, t)$ to zero at $z = 0$, matching the boundary condition (2). The $a_0(t)z/g$ term represents the field caused by the average value of $f(x)$. The remaining coefficients $a_n(t)$ are found in the usual manner for Fourier series by multiplying both sides of Eq. (3) by $(\cos k_m x)/x_0$ and integrating over x from 0 to x_0 . Only for $m = n$ will the right-hand side yield a nonzero integral, resulting in

$$a_n(t) = \frac{2V_s(t)}{x_0 \sinh k_n g} \int_{x=0}^{x_0} f(x) \cos k_n x dx \quad (4)$$

Performing the integral in Eq. (4) while using the potential function $f(x)$ of Fig. 6a results, after some algebra, in

$$a_n(t) = \frac{4V_s(t)}{x_0 k_n \sinh k_n g} \sin(Wk_n/2) \quad (5)$$

Here, W is the width of a single finger electrode, and $V_s(t)$ again is the sinusoidal voltage applied to the signal fingers. The value of the coefficient a_0 in Eq. (3) is found by taking the spatial average of $f(x)$, yielding:

$$a_0 = \frac{V_s(t)W}{x_0} \quad (6)$$

Computing the charge induced on the sense fingers requires an expression for the normal electric field E_z along

Table 1
Actuator and electrode specifications

<i>Actuator</i>	
Length	350 μm
Width	350 μm
Gap spacing	2 μm
<i>Interdigitated electrodes</i>	
Active length	350 μm
Width	5 μm
Spacing	2 μm
Number of finger pairs	24
<i>Signal voltage</i>	
Frequency	260 kHz
Peak amplitude	4.6 V
<i>Amplifier</i>	
I/V conversion ratio	10^6
Input resistance	1 m Ω
Measured bandwidth	300 kHz
Op-amp type	LF411

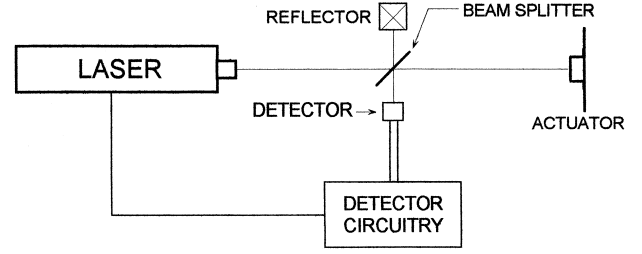


Fig. 7. Laser doppler interferometer system used to measure actuator position independently.

the electrode plane at $z = g$. The latter is readily obtained from the fundamental definition $E = -\nabla\Phi$, yielding

$$E_z = -\frac{\partial\Phi}{\partial z} = -\frac{a_0(t)}{g} - \sum_{n=1}^{\infty} a_n(t) k_n \cos k_n x \cosh k_n g \quad (7)$$

The surface charge density induced on the sense fingers will be equal to $\epsilon_0 E_z$. The total charge Q induced on the sense electrodes can be found by integrating $\epsilon_0 E_z$ over the area of the sense fingers:

$$Q = NL\epsilon_0 \int_b^{x_0-b} E_z dx \quad (8)$$

where W is again the width of a single sense finger, d the distance between fingers, and $b = W/2 + d$. The dimension L describes the active finger length (the portion of finger length under the actuator diaphragm), and N is the total number of signal-sense finger pairs. Computing the integral specified in Eq. (8) results in:

$$Q(t) = NL\epsilon_0 \left[\frac{a_0(t)}{g} (2b - x_0) \times \sum_{n=1}^{\infty} 2a_n(t) \cosh k_n g \sin k_n b \right] \quad (9)$$

The current flowing to the sense electrodes in response to $V_s(t)$ can be found from $i(t) = dQ(t)/dt$. For a $V_s(t)$ that is sinusoidal in time, the magnitude of $i(t)$ will be equal to ω times the magnitude of Q , where ω is the frequency of $V_s(t)$ in radians per second. If the current-to-voltage converter of Fig. 3 receives $i(t)$ as its input, its output signal voltage will given by

$$v(t) = N\omega RL\epsilon_0 \left[\frac{a_0(t)}{g} (2b - x_0) \times \sum_{n=1}^{\infty} 2a_n(t) \cosh k_n g \sin k_n b \right] \quad (10)$$

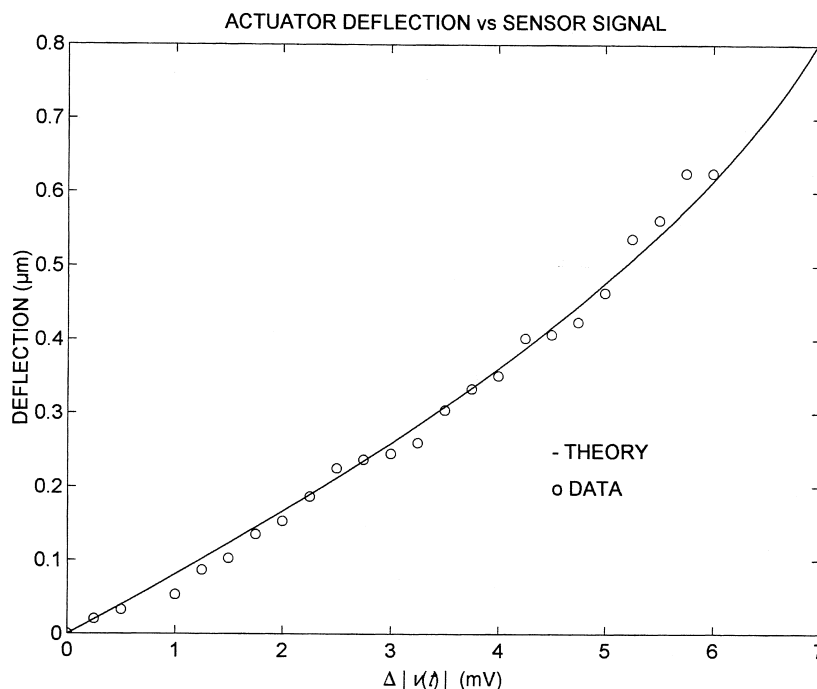


Fig. 8. Plots of deflection vs. change in sensor output voltage. Dots: measured values of position vs. $\Delta|v(t)|$. Solid line: theoretical prediction based on Eq. (10).

where R is the feedback resistor in Fig. 3. Note that $v(t)$ in Eq. (10) is a function of the actuator gap spacing g and thus forms the basis for sensing actuator deflection.

4. Experimental verification

A capacitive sensing system of the type depicted in Fig. 3 was tested on a single actuator having the parameters listed in Table 1. The width and spacing of the interdigitated electrodes were chosen based on field analysis to maximize the induced signal charge while staying within the bounds of MUMPS design rules and fabrication limits. The current-to-voltage converter was fabricated from a single, inexpensive, off-the-shelf LF411 op-amp an ordinary 5% tolerance 1/4-W resistor. Actuator deflection was measured independently using a Zygo laser doppler interferometer system, as illustrated in Fig. 7. The results are plotted in Fig. 8. The circles in Fig. 8 show the measured actuator deflection as a function of $\Delta|v(t)|$, where $\Delta|v(t)|$ represents the change in the peak value of the voltage at the output of the current-to-voltage converter. The values have been multiplied by an arbitrary scaling factor of 200. The solid line in Fig. 8 represents the curve predicted by summing the first one hundred terms of the infinite series in Eq. (10). The theoretical curve and experimental data exhibit the same shape, suggesting that the sensor is operating as expected.

When a signal voltage is applied to the interdigitated electrodes, stray coupling between the wire interconnects

leading to the MEMS chip can cause an unwanted signal voltage component to appear at the current-to-voltage converter. This unwanted signal voltage must be subtracted from the deflection-sensitive $v(t)$ before the data can be interpreted. The meaningful signal quantity is therefore the *change* in peak output signal voltage as a function of actuator deflection. In our case, the stray signal was on the order of 4 V p-p, while the measured signal was on the order of millivolts.

5. Improved sensor with linear response

For the coordinate system of Fig. 6a, the infinite series solution (3) is valid for any arbitrary potential boundary condition $f(x)$ at $z = g$. The alternative $f(x)$ of Fig. 9 has a linear, rather than step, variation in voltage between signal and sense fingers. By choosing this alternative $f(x)$, the voltage output of the sensor can be made to be a linear function of gap spacing g . In practice, the $f(x)$ of Fig. 9 could be achieved by depositing uniformly resistive mate-

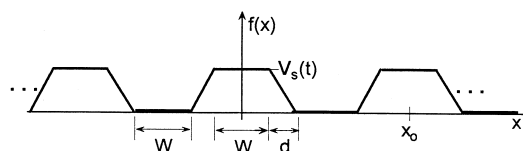


Fig. 9. Alternative potential boundary condition $f(x)$ with linear voltage variation between signal and sense fingers.

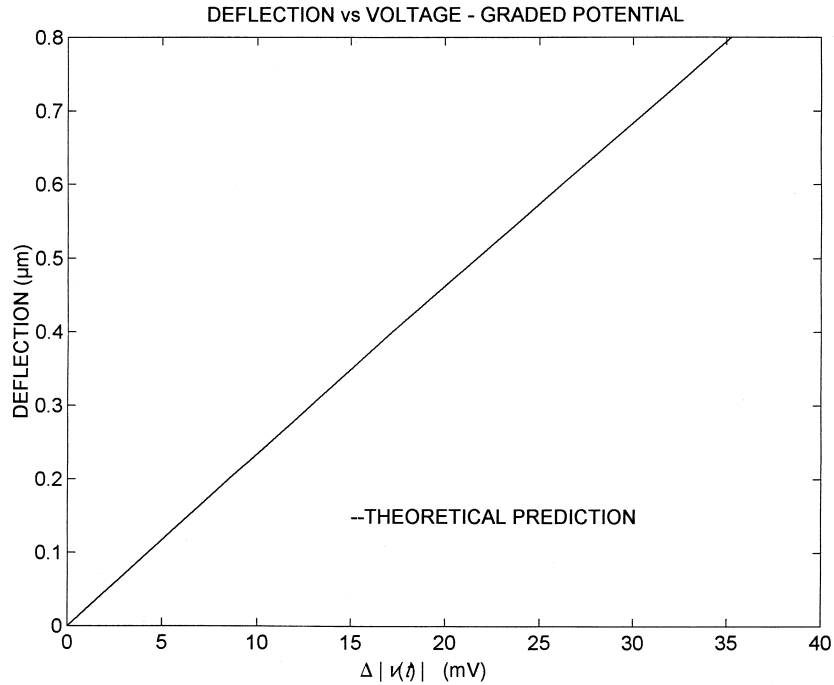


Fig. 10. Theoretical $\Delta|v(t)|$ vs. position curve for the alternative potential boundary condition $f(x)$ of Fig. 9.

rial between the fingers. The modified Fourier coefficients $a_n(t)$ computed using Eq. (4) become, after some algebra,

$$a_n(t) = \frac{4V_s(t)}{x_0(b - W/2)k_n^2 \sinh k_n g} (\cos k_n W/2 - \cos k_n b) \quad (11)$$

and

$$a_0(t) = \frac{V_s(t)}{x_0} (W/2 + b) \quad (12)$$

where again $b = W/2 + d$. Substituting these coefficients into Eq. (10) and summing the first one hundred terms of the series leads to the theoretical $\Delta|v_s(t)|$ vs. deflection plot of Fig. 10. This plot is linear, suggesting that the resistive gradation of voltage between the interdigitated electrode fingers compensates for the nonlinearity inherent to the spatial harmonic components of the field distribution. The predicted sensor signal is also much larger than that obtained for the theoretical and experimental $f(x)$ of Fig. 6 because a higher field flux per unit signal voltage terminates on the sense fingers.

6. Conclusion

A differential capacitive position sensor based on interdigitated finger electrodes has been developed for use with MEMS structures involving motion perpendicular to the substrate plane. The system provides a simple way of monitoring actuator deflection using inexpensive off-the-shelf electronic components and has been demonstrated using double-anchored, bridge-type MEMS actuators. In

this application, the sensing system can be implemented by building sense electrodes only beneath the moving actuator diaphragm while permitting the actuator diaphragm to be connected directly to ground. These features are essential to the development of optically perfect deformable mirror arrays. By linearly grading the voltage distribution in the space between driven and sensing finger electrodes, the voltage vs. deflection response can be made linear.

Acknowledgements

Thanks to Raji Krishnamoorthy-Mali for her help in fabricating the devices and in taking the experimental data. This work was supported by the U.S. Defense Advanced Research Projects Administration (DARPA) under Grant No. DABT 63-95-C-0065.

References

- [1] R. Krishnamoorthy Mali, T. Bifano, M. Horenstein, N. Vandelli, Development of microelectromechanical deformable mirrors for phase modulation of light, *Opt. Eng.* 36 (2) (1997) 542–548.
- [2] T.G. Bifano, R. Krishnamoorthy-Mali, J. Dorton, J. Perreault, N. Vandelli, M. Horenstein, D. Castanon, Continuous-membrane surface-micromachined silicon deformable mirror, *Opt. Eng.* 36 (5) (1997) 1354–1360.
- [3] M. Horenstein, T. Bifano, R. Krishnamoorthy Mali, N. Vandelli, Electrostatic effects in micromachined actuators for adaptive optics, *J. Electrostat.* 42 (1/2) (1997).
- [4] G.K. Fedder, R.T. Howe, Multimode digital control of a suspended polysilicon microstructure, *J. Microelectromech. Syst.* 5 (4) (1996) 283–297.

- [5] G.K. Fedder, R.T. Howe, Integrated test bed for multi-mode digital control of suspended microstructures, Tech. Digest Solid-State Sensor and Actuator Workshop, Hilton Head, SC, June 1994, pp. 145–150.
- [6] C. Lu, M. Lemkin, B.E. Boser, A monolithic surface micromachined accelerometer with digital output, IEEE J. Solid-State Circuits 30 (12) (1995) 1367–1373.
- [7] W. Yun, R.T. How, P.R. Gray, Surface micromachined digitally force-balanced accelerometer with integrated cmos detection circuitry, Tech. Digest Solid-State Sensor and Actuator Workshop, Hilton Head, SC, June 1992, pp. 21–25.
- [8] 15. D. Koester, R. Mahadevan, K.W. Markus, MUMPs Introduction and Design Rules, MCNC Technology Applications Center, 3021 Cornwallis Road, Research Triangle Park, NC, Oct. 1994 (<http://mems.mcnc.org/mumps.html>).
- [9] M. Zahn, Electromagnetic Field Theory, Wiley, New York, 1979.
- [10] D. Cheng, Field and Wave Electromagnetics, Addison-Wesley, Reading, MA, 1989.

Mark N. Horenstein received his SB and PhD degrees in electrical engineering from the Massachusetts Institute of Technology in 1973 and 1978, respectively, and his MS degree in electrical engineering from the University of California at Berkeley in 1975. From 1978 to 1979, he was a research scientist and development engineer for Spire in Bedford, MA. In 1979, he joined the faculty in the Department of Electrical and Computer Engineering at Boston University where he leads the Laboratory for Applied Electromagnetics. He specializes in the field of electrostatics and its application to problems in research and industry. He is the author of numerous papers on topics in electrostatics, including the development of electric field and ion measuring instrumentation and charge neutralization, and he holds several patents related to electrostatic devices and processes. He also is the author of the widely used textbook, *Microelectronic Circuits and Devices*. He has worked with the Boston University MEMS team since 1995.

Julie A. Perreault received her BS degree in electrical engineering from Boston University in 1996. She also has worked as a design engineer at P&E Microcomputer Systems on research and development tools for microprocessors. She is currently in the PhD program in electrical engineering at Boston University. She is interested in the application of microprocessors to control systems and is working on position sensing technology for micro-electromechanical structures.

Thomas G. Bifano received BS and MS degrees in mechanical engineering and materials science from Duke University in 1980 and 1983, respectively, and a PhD in 1988 in mechanical engineering from North Carolina State University. Since joining the faculty of Boston University in 1988, he has developed an internationally known research program to study ultraprecision machining. He directs the Boston University Precision Engineering Research Laboratory, where currently he oversees projects on ion machining of ceramics and MEMS devices, hard-disk substrate fabrication, and silicon micromachining of deformable mirror systems.